Japanese Journal of Applied Physics

Low-Loss Si Wire Waveguides and their Application to Thermooptic Switches

To cite this article: Tai Tsuchizawa *et al* 2006 *Jpn. J. Appl. Phys.* **45** 6658

Japanese Journal of Applied Physics
Vol. 45, No. 8B, 2006, pp. 6658–6662

Low-Loss Si Wire Waveguides and their Application to Thermooptic Switches

Tai TSUCHIZAWA, Koji YAMADA, Hiroshi FUKUDA, Toshifumi WATANABE,
Shingo UCHIYAMA and Seiichi ITABASHI

NTT Microsystem Integration Laboratories, 3-1 Morinosato Wakamiya, Atsugi, Kanagawa 243-0198, Japan

(Received January 16, 2006; accepted March 15, 2006; published online August 22, 2006)

We demonstrate low-loss Si wire waveguides with good thermal stability and thermooptic (TO) switches made from them. The propagation losses of the fabricated waveguides were around 2 dB/cm and the coupling losses to an external fiber were 0.4 dB. These values were achieved by improving the fabrication process and introducing spot-size converters made from inorganic materials. Using these waveguides, we made two types of TO switches, a 1×1 switch with a multimode interference (MMI) branch and a 2×2 switch with a 3-dB directional coupler. Both switches exhibited a high extinction ratio of more than 30 dB at a low electric power of 30 mW and a switching time shorter than 200 µs.

[DOI: 10.1143/JJAP.45.6658]

KEYWORDS: Si wire waveguide, high refractive-index contrast, spot-size converter, branch, MMI, directional coupler, TO switch

1. Introduction

Future optical network systems will require economical multifunctional optical devices with a low power consumption. The key to achieving multiple functions is to miniaturize and integrate various kinds of passive and functional optical devices. Reducing the size of optical devices will also lower their power consumption.

Silicon wire waveguides based on silicon-on-insulator (SOI) structures are a promising for highly integrated, ultrasmall optical devices.[1–5] Due to their very high refractive-index contrast and strong confinement, they have a core size of less than 1 µm for single-mode propagation and sharp bends with bending radii of only a few micrometers are possible. These features should enable us to make optical circuits that are ultrasmall and have high integration densities, and also to utilize nonlinear effects that are enhanced by high power density. It is also possible to integrate Si wire waveguides with Si electronic circuits. This could lead to new functional optical devices that are electrically controlled, and could yield convergent electronic-photonic devices.

However, the key handicaps of Si wire waveguides were their high coupling loss with external fibers and high propagation loss. We have resolved the high coupling loss problem by introducing a spot-size converter that consists of a Si inverse taper and a low-index polymer waveguide.[6] The propagation loss has been improved largely by reducing the sidewall roughness of the Si core.[5,7] Optical devices with advanced functionality can now be designed using the Si wire waveguides.

In this paper, we demonstrate Si wire-based microswitches utilizing a thermooptic (TO) effect. The TO effect of Si is about tenfold larger than that of silica. This means that the refractive index of Si is highly dependent on temperature. Therefore, the Si-based TO switch can be expected to significantly reduce the electrical power consumption of switching operations.[8] First, we describe the fabrication of low-loss Si wire waveguides with spot-size converters made from inorganic materials to improve thermal stability. Then, we show the results from fabricated branches that constitute the basic part of a TO switch, and finally discuss the switching characteristics.

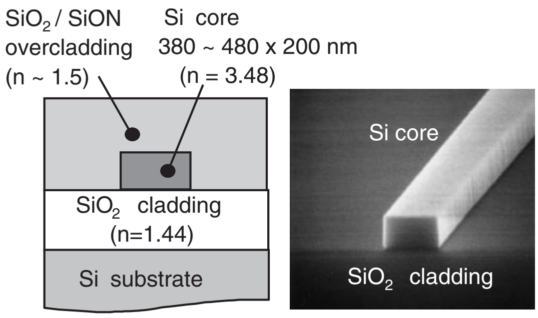

Fig. 1. Structure of Si wire waveguide.

2. Experimental Procedure

2.1 Waveguide structure

Si wire waveguides were fabricated on SOI wafers with a 200 nm Si top layer and a 3 µm buried SiO_2 layer. The cross-sectional structure of the waveguide is shown in Fig. 1. The core size is 380–480 by 200 nm which can provide a single-mode propagation for practical use at communication wavelengths of around 1.5 µm. The thick buried SiO_2 layer works as the undercladding and reduces losses due to leakage to the Si substrate. For efficient connection to an external fiber, we placed spot-size converters at each end of the Si wire waveguide. Figure 2 shows the structure of the spot-size converter. The converter consists of a Si taper that gradually becomes thinner toward the end and a second low-index waveguide that covers the taper. The Si taper is 300 µm long, and the tip of the taper is 80 nm wide. In this study, the low-index waveguides were made from a SiO_xN_y core and a SiO_2 cladding. We changed the material of low-index waveguides from polymer to inorganic materials to achieve high thermal stability. The core size is about 3 µm square and the index contrast is about 3%. This converter also has high durability to high-power optical inputs with high thermal stability because it is made of inorganic materials.[9]

2.2 Fabrication process

The following is the fabrication process for Si wire waveguides. First, a SiO_2 film is deposited on the surface Si layer of the SOI wafer by plasma-enhanced chemical vapor

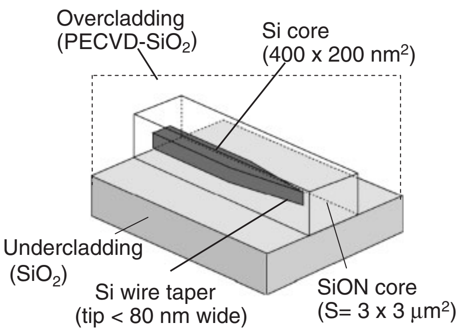

Fig. 2. Schematic of spot-size converter made from inorganic materials.

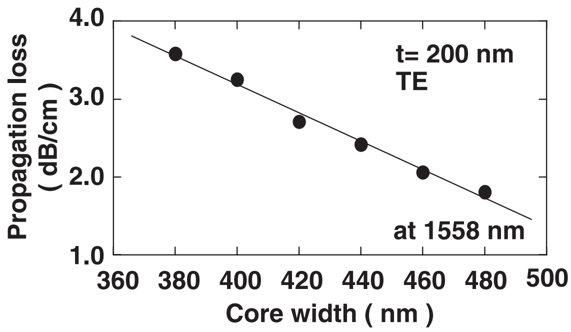

Fig. 4. Propagation loss of Si wire waveguide with 200 nm high core as function of core width.

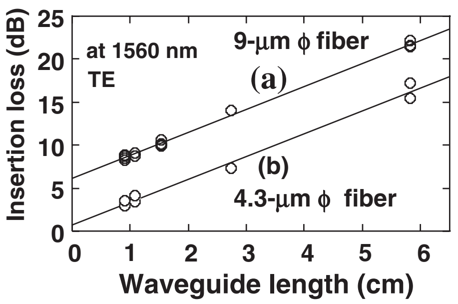

Fig. 3. Insertion loss for TE mode of Si wire waveguide ranging in length from 0.9 to 5.8 cm. These are measured at 1560 nm using (a) a conventional single-mode fiber with a 9 μm mode-field diameter and (b) a fiber with a 4.3 μm mode-field diameter.

deposition (PECVD) as a hard mask for Si etching. Next, the resist patterns that will become the Si core and taper for the spot-size converter are formed by e-beam (EB) lithography, in which a variable-shaped EB writer, EB-X3, was used.[10] Then, the SiO_2 hard mask pattern for Si etching is formed by reactive ion etching (RIE), and is transferred to the Si layer using electron cyclotron resonance (ECR) plasma etching with fluoride gases. Next, a 3-μm-thick SiO_xN_y film for the spot-size converter is deposited on the Si waveguide by PECVD. Then, the SiO_xN_y core is formed on the Si taper by photolithography and RIE. The SiO_xN_y film on the Si wire core was not etched off so that the Si core would not be damaged during SiO_xN_y etching. Finally, the wafer is coated with 5-μm-thick PECVD SiO_2 as the overcladding. In addition, for TO switch fabrication, a thin metal film is deposited on the overcladding by ion beam sputtering and thin film heaters are fabricated by ion milling.

3. Results and Discussion

3.1 Fundamental characteristics of Si wire waveguides

We measured the insertion losses of the Si wire waveguides of different lengths to evaluate the propagation and coupling losses. Figure 3 shows the insertion loss of the Si wire waveguide for the transverse electric (TE) mode (the electric field vector parallel to the substrate), as a function of the waveguide length. Lines (a) and (b) are for the conventional single-mode fiber with a 9 μm mode-field diameter and the fiber with a 4.3 μm mode-field diameter, respectively. The waveguides have $420 \times 200\,\mathrm{nm}^2$ core sizes and spot-size converters at both ends. The fibers were butt-coupled to the SiO_xN_y low-index waveguide of the spot-size converter for these measurements. The slope of these lines yields the propagation loss of the Si wire waveguide. The propagation loss was calculated to be 2.6 dB/cm from the slope of the fitted line. This low propagation loss was obtained because the sidewall roughness of the Si core was reduced. To form very smooth sidewalls, we improved the EB data preparation and writing methods because the sidewall roughness is mainly introduced due to imperfections in the resist pattern.[11] Using a transmission electron microscopy (TEM) image, the rms roughness of the sidewall was estimated to be less than 2 nm.[12] The y-intercept of the line in this figure shows the coupling loss for two converters. We estimated the coupling loss for one converter to be 0.4 dB for the 4.3 μm mode-field fiber, and 3.0 dB for the 9 μm mode-field conventional fiber.

Figure 4 shows how the propagation loss of the Si wire waveguide with the 200-nm-high core depends on core width. Propagation loss decreases with increasing core width, and was reduced to less than 2 dB/cm at a 480 nm core width. This result indicates that propagation loss can be reduced by adjusting the shape of the core. An increase of core width yields an increase in the distance to the sidewalls such that the influence of the sidewall should decrease. We think this is the reason the loss is reduced in the extended core. The loss of about 2 dB/cm is low enough for practical applications, because Si wire-based photonic devices can be constructed with very short waveguides.

Figure 5 shows the transmission spectrum of a Si wire waveguide with spot-size converters made of SiO_xN_y. The absorption near 1500 nm due to NH in SiO_xN_y is weak. Therefore, the applicable bandwidth of the Si wire waveguide with the SiO_xN_y converter is larger than 250 nm. Moreover, there are no significant Fabry–Perot ripples in the transmission spectrum, which means that there is little reflection at the spot-size converter. The dip near 1500 nm due to NH can be excluded by making the converter of Si-rich oxide, SiO_x, instead of SiO_xN_y.

3.2 Branches

Branches in optical waveguiding systems are indispensable for constructing interferometers. First, we have developed two types of branches on the basis of multimode interference (MMI) and a directional coupler, which are used to make thermooptic switches.

Figure 6 shows a scanning electron microscopy (SEM) image of a fabricated MMI branch for Si wire waveguides

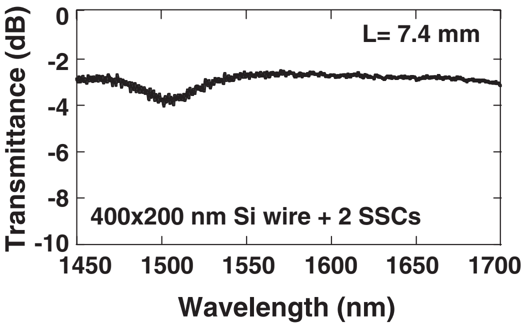

Fig. 5. Transmission spectrum of 7.4-mm-long Si wire waveguide with spot-size converters made of SiO_xN_y. The dip near 1500 nm is due to NH absorption in SiO_xN_y.

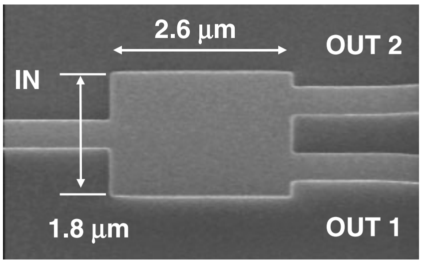

Fig. 6. SEM image of fabricated MMI branch for Si wire waveguides with $400 \times 200\,nm^2$ cores.

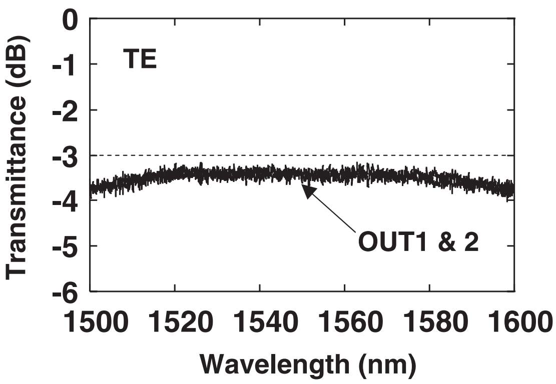

Fig. 7. Transmission spectra of MMI branch for TE mode. The spectra were calibrated using a neighboring Si wire whose length was the same as that of the MMI branch.

with 400×200-nm^2 cores. The branch consists of a simple rectangle $2.6 \times 1.8\,\mu m^2$ and three waveguide ports. As this branch has no steep structure, an accurate fabrication can be performed. Figure 7 shows the transmission spectra of a MMI branch for a TE mode. The spectra were calibrated by a neighboring simple Si wire sample whose length was the same as that of the sample with the MMI branches. As shown, the spectra of both ports agreed very well and were almost flat within a 100 nm wavelength range. Furthermore, the excess losses were as small as about 0.4 dB. This MMI branch already exhibits excellent characteristics.

Figure 8 shows a SEM image of a fabricated directional coupler. The coupler length is 13.75 μm, and the coupler gap is 310 nm. The size of the waveguide core is $400 \times 200\,nm^2$. The ends turn sharply away from each other with a small

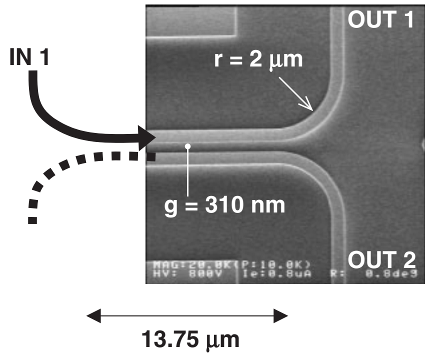

Fig. 8. SEM image of fabricated directional coupler for Si wire waveguides with $400 \times 200\,nm^2$ cores. The coupling length is 13.75 μm, and the coupler gap is 310 nm.

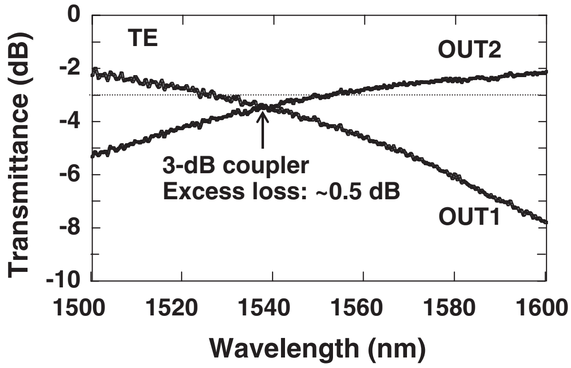

Fig. 9. Transmission spectra of directional coupler for TE mode. The spectra were calibrated using a neighboring Si wire whose length was the same as that of the directional coupler.

bending radius of only 2 μm in order to quickly separate the waveguides and reduce excess coupling. Figure 9 shows the transmission spectra of a coupler for a TE mode. As shown, the spectra are typical for a directional coupler. At a 1538 nm wavelength, the coupler works as a 3-dB coupler. The excess loss was about 0.5 dB, which was mainly caused by the loss of the bend with the ultrasmall radius of 2 μm.[5)]

3.3 Thermooptic switch

We fabricated TO switches using the developed branches and evaluated their characteristics. We made two types of TO switches, a 1×1 switch with an MMI branch and a 2×2 switch with a 3-dB directional coupler using Si wire waveguides with $400 \times 200\,nm^2$ cores. Figure 10 shows the structures of the fabricated TO switches. Each switch is basically a Mach–Zehnder interferometer consisting of two branches and waveguide arms equipped with thin-film heaters to control the refractive index. One switch element is about $650 \times 200\,\mu m^2$. The electric heater on the waveguides is 450 μm long and the cross section is 5 μm wide and 0.2 μm high. It was made of a Au-based alloy. The heaters are constructed on the overcladding, which is 8 μm thick.

Figure 11 shows output power versus applied electric power for the 1×1 and 2×2 switches. These measurements were performed for the TE mode at 1532 nm using the fiber with a 9 μm mode-field diameter. The fiber was

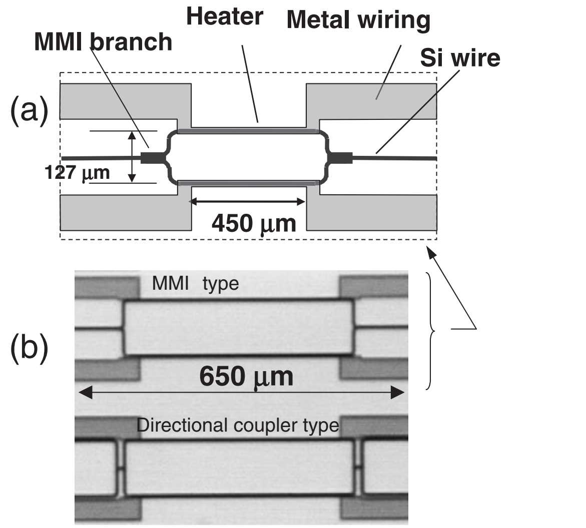

Fig. 10. (a) Schematic of 1×1 TO switch structure and (b) optical microscope image of fabricated 1×1 and 2×2 TO switches. The length between the two waveguide arms is 127 μm and the electric heater on the waveguides is 450 μm long.

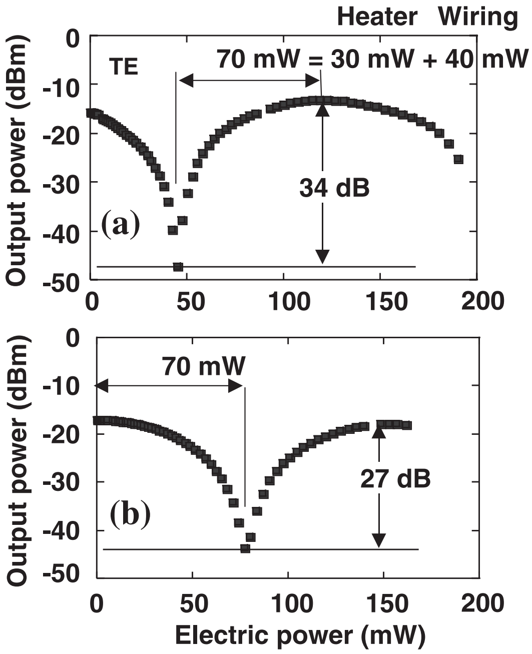

Fig. 11. Output power vs applied electric power for (a) 1×1 switch and (b) 2×2 switch.

connected to the SiO_xN_y waveguide of the spot-size converter with a 20 μm joint gap for movement. At an applied power of 70 mW, we obtained very high extinction ratios of 34 dB for the 1×1 switch and 27 dB for the 2×2 switch. The electric power needed for this switching operation was estimated to be as low as 30 mW, because the powers consumed at the heater and the wiring part were estimated to be 30 and 40 mW, respectively, from the ratio of the electric resistance. These TO switches should have the potential to provide switching operations with a low power consumption below 10 mW if additional structures such as heat insulating grooves are added.[13] The low-power switching operations are due to the high TO effect of the Si and the

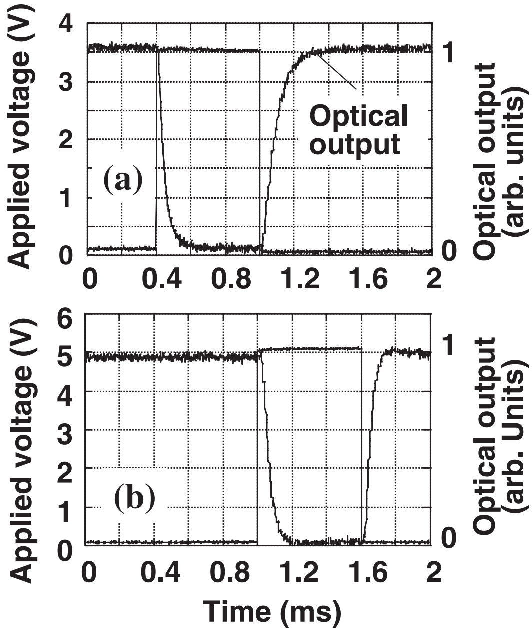

Fig. 12. Optical switching response of TO switch when 3.5 V square-wave pulsed voltage of with 600 μs width was applied. (a) 1×1 switch and (b) 2×2 switch.

reduction in switch size due to the Si wire waveguide. The insertion losses were about 13 dB for both switches. These losses were broken down into the propagation loss of the Si wire waveguide (2 dB/0.6 cm), the coupling loss between the fiber and the waveguide (10 dB/two connections) and the branch loss in the switch device (1 dB/two branches).

Figure 12 shows the optical switching response of the TO switch when a square-wave pulsed voltage of 3.5 V with a 600 μs width was applied. For the 1×1 and 2×2 switches, the rise and fall times are both less than 200 μs (Fig. 12). This value is very fast for a TO switch and is about tenfold faster than those for a conventional silica-based TO switch.[12] The fast switching operation of the Si wire-based TO switch comes from the thinness of the cladding layer, which enables the waveguide to quickly heat up and allows heat to rapidly dissipate into the Si substrate.

4. Conclusions

We developed a low-loss Si wire waveguide with good thermal stability by improving the fabrication processes and using a spot-size converter made of inorganic materials. The propagation loss was as low as 2 dB/cm and the coupling loss to an external fiber was 0.4 dB. An MMI branch and a 3-dB directional coupler, which are the basic parts of an interferometer, were made from the new waveguide. They exhibited excellent branch characteristics with sufficiently low excess loss. We used these branches to make TO switches based on a Mach–Zehnder interferometer, and examined the switching characteristics. For 1×1 and 2×2 switches, we obtained an extinction ratio of more than 30 dB, a low electrical power consumption of 30 mW, and a switching time shorter than 200 μs.

Acknowledgment

The authors would like to thank Hirofumi Morita, Junichi Takahashi, and Mitsutoshi Takahashi for useful discussions.

1) L. C. Kimerling: Appl. Surf. Sci. **159–160** (2000) 8.
2) A. Sakai, T. Fukazawa and T. Baba: IEICE Trans. Electron. **E85-C** (2002) 1033.
3) K. Yamada, T. Tsuchizawa, T. Watanabe, J. Takahashi, E. Tamechika, M. Takahashi, S. Uchiyama, H. Fukuda, T. Shoji, S. Itabashi and H. Morita: IEICE Trans. Electron. **E87-C** (2004) 351.
4) W. Bogaerts, R. Baets, P. Dumon, V. Wiaux, S. Beckx, D. Taillaert, B. Luyssaert, J. V. Campenhout, P. Bienstman and D. V. Thourhout: J. Lightwave Technol. **23** (2005) 401.
5) T. Tsuchizawa, K. Yamada, H. Fukuda, T. Watanabe, J. Takahashi, M. Takahashi, T. Shoji, E. Tamechika, S. Itabashi and H. Morita: IEEE J. Sel. Top. Quantum Electron. **11** (2005) 232.
6) T. Shoji, T. Tsuchizawa, T. Watanabe, K. Yamada and H. Morita: Electron. Lett. **38** (2002) 1669.
7) Y. A. Vlasov and S. J. McNab: Opt. Express **12** (2004) 1622.
8) T. Chu, H. Yamada, S, Ishida and Y. Arakawa: Opt. Express **13** (2005) 10109.
9) H. Fukuda, K. Yamada. T. Shoji, M. Takahashi, T. Tsuchizawa, T. Watanabe, J. Takahashi and S. Itabashi: Opt. Express **13** (2005) 4629.
10) T. Morosawa, K. Saito, Y. Takeda, T. Kunioka, A. Shimiza, J. Kato, T. Matsuda, Y. Kuriyama, Y. Nakayama and Y. Matsui: J. Vac. Sci. Technol. B **17** (1999) 2907.
11) T. Watanabe, T. Tsuchizawa, K. Yamada, H. Fukuda and S. Itabashi: Proc. Int. Conf. Microprocesses and Nanotechnology, Tokyo, 2005, p. 240.
12) J. Takahashi, T. Tsuchizawa, T. Watanabe and S. Itabashi: J. Vac. Sci. Technol. B **22** (2004) 2522.
13) R. Kasahara, M. Yanagisawa, A. Sugita, T. Goh, M. Yasu, A. Himeno and S. Matsui: IEEE Photonics Technol. Lett. **11** (1999) 1132.